# New chemical tools to illuminate N-acylphosphatidylethanolamine biosynthesis

Wendel, T.J.

# 6

# Development of potent and selective ABHD6 inhibitors based on caged hydrocarbon structures

Since its discovery in 1933[1], adamantane, an organic compound consisting of three fused cyclohexanes in their chair conformation ($(CH)_4(CH_2)_6$, **1**, Figure 6.1), has intrigued chemists due to its physicochemical and biological properties.[2,3] Named after the Greek *adamantinos*, meaning diamond-related, it is the simplest member of the family of caged hydrocarbons that have their carbon atoms in a diamond-like lattice arrangement (named diamondoids), which gives them an extraordinarily rigid and almost strain-free structure.[2,4] Initially, adamantane could only be isolated from petroleum, which limited the possibilities for derivatization and its widespread use. The first convenient synthesis published in 1957 opened up the possibilities for its application in medicinal chemistry.[5] Derivatives such as amantadine (**2**), memantine (**3**) and vildagliptin (**4**) have since entered the clinic for the treatment of viral infections, diabetes mellitus and neurodegenerative diseases such as Alzheimer's and Parkinson's disease (Figure 6.1).[3,6–12]

Diamondoids are lipophilic moieties. Inhibitors with an adamantyl group, however, have a lower lipophilicity than their cyclohexyl counterparts, as determined by their octanol–water partition coefficient (logP).[13] Adamantane has therefore been dubbed the 'lipophilic bullet', providing a compact moiety of critical hydrophobicity to a drug.[3] For this reason, adamantane has been used as a fatty acid-mimic in peroxisome proliferator-activated receptor (PPAR) pan-agonists[14] and as cell membrane anchor in glucosylceramidase inhibitors.[15–17] It has also been incorporated in various drug candidates to increase their water solubility[18], improve brain-penetration[19] or to increase their selectivity.[20] Its hydrophobicity may, however, negatively impact oral bioavailability, but increase the volume of distribution and half-life.[21,22] The rigidity and bulkiness of adamantane may improve the metabolic stability of a drug by inducing steric hindrance.[6,23,24] Importantly, combination of these beneficial properties is not easily obtained by using more conventional structures.[25–27]

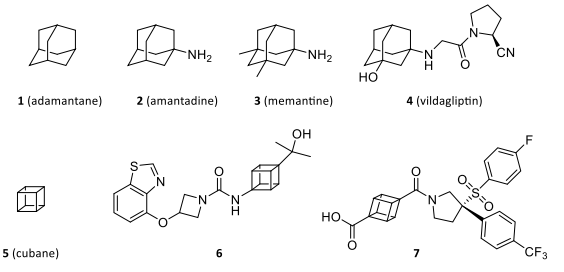


**Figure 6.1. Examples of caged hydrocarbons and their use in published drugs.** Adamantane is the smallest representative of the diamondoid class. Amantadine has been used as antiviral and for the treatment of Parkinson's disease[62], memantine for the treatment of Alzheimer's disease[7], vildagliptin is used as anti-diabetic.[12] Cubane is another small caged hydrocarbon that was used in this study. Compound **6** has been published as an inhibitor of prostaglandin D synthase, **7** is a retinoid-related orphan receptor γ ligand.[28]

Following the increased use of adamantane, other caged hydrocarbons such as cubanes have also been leveraged by medicinal chemists (**5**–**7**, Figure 6.1). The size of a cubyl group (2.72 Å) is almost identical to that of a phenyl (2.79 Å), making it a potential bioisoster for this commonly applied functional group in drug discovery. A clear advantage of cubane is its three-dimensional structure which allows for derivatization in different exit vectors compared to the phenyl ring. In addition, the cubyl group is highly stable towards light, heat and oxidation.[28,29] Its widespread use is, however, hampered by a lack of readily available building blocks.[30]

Serine hydrolases (SHs), a superfamily of enzymes characterized by the presence of a catalytic serine used for substrate hydrolysis, play key roles in multiple (patho)physiological processes, including coagulation, neurotransmission, hypertension, cancer and neuroinflammation.[31–33] They are important drug targets, and currently over ten SH inhibitors have entered the clinic.[32] Several SHs, such as diacylglycerol lipases α and β (DAGLα and DAGLβ) and α/β hydrolase domain-containing proteins 6 and 16a (ABHD6 and ABHD16a), are potential targets for the treatment of neurological diseases associated with neuroinflammation. DAGLα and DAGLβ hydrolyze diacylglycerols into free fatty acids and monoacylglycerols, including 2-arachidonoyl glycerol (2-AG), an endogenous agonist of the cannabinoid $CB_1$ and $CB_2$ receptors.[31,34] It is also an intermediate in the formation of pro-inflammatory lipids, such as prostaglandins and eicosanoids.[34–37] ABHD6 converts di- and monoacylglycerols into free fatty acids and glycerol and participates in both production and degradation of 2-AG.[38] It has recently been suggested as potential drug target in microglial cells that play a fundamental function in the development of neuroinflammation[39–42], including for the treatment of traumatic brain injury[43] and multiple sclerosis.[44–46] Of note, while several ABHD6 inhibitors have been developed, their off-target effects have hampered this research.[44,47] ABHD16a is a phosphatidyl serine (PS) lipase producing lyso-PS in the brain. This lipid mediator is involved in several pathways of inflammatory responses, and elevated levels caused by attenuated degradation are the hallmark of the neurological disorder polyneuropathy, hearing loss, ataxia, retinitis pigmentosa, cataract (PHARC).[48–50] Inhibition of ABHD16a may therefore provide a treatment opportunity for PHARC patients.

For both DAGL and ABHD6 various inhibitors have been developed and shown to exhibit potent inhibition in cellular and animal models of neuroinflammation (**8**–**11**, Figure 6.2).[34,51–54] ABHD16a can be inhibited by XGN067 (**12**).[55] These inhibitors belong to the class of triazole ureas and contain an electrophilic carbonyl that covalently binds to the catalytic serine of SHs, with the triazole functioning as leaving group. KT109 (**8**), DH376 (**9**) and AJ126 (**10**) were developed as DAGL inhibitors, but cross-reactivity was observed with ABHD6, whereas XGN067 was shown to target multiple enzymes beside ABHD16a.[54–56] KT182 (**11**) is a highly potent, *in vivo* active ABHD6 inhibitor which has been used to study the role of ABHD6 in neuroinflammation[44,46], but its off-targets include FAAH, the enzyme responsible for the degradation of anandamide (*N*-arachidonoyl ethanolamine, AEA), the

second major CB receptor agonist.[53,57] Improving the selectivity of these inhibitors would aid in the development of compounds that specifically modulate the desired physiological function of the targeted enzyme. In this chapter, a set of triazole urea-based compounds with caged hydrocarbon substituents were synthesized to investigate their effect on the activity and selectivity of these lipase inhibitors.

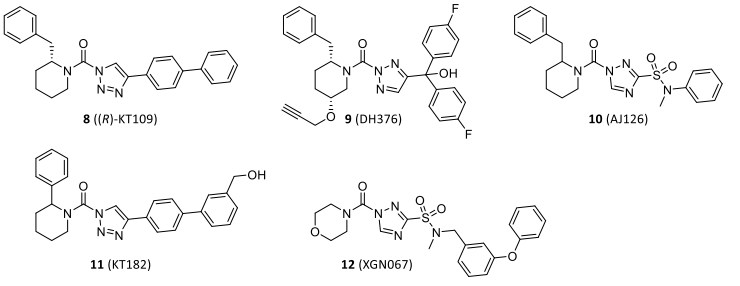


**Figure 6.2. Chemical structures of some previously published DAGL, ABHD6 and ABHD16a inhibitors.** 2-Benzylpiperidine-containing compounds KT109, DH376 and AJ126 were reported as DAGL or dual DAGL/ABHD6 inhibitors[52,54,56,59,63], 2-phenylpiperidine-containing compound KT182 was reported as ABHD6 inhibitor.[53] Morpholine-containing XGN067 was reported as ABHD16a inhibitor.[55]

## Results and discussion

### Design and synthesis of compounds 13–21

The DAGL, ABHD6 and ABHD16a inhibitors outlined in Figure 6.2 feature lipophilic phenyl moieties in the triazole leaving group. These phenyl groups make important hydrophobic interactions with their respective enzymes[53,56] and were replaced with a caged hydrocarbon as a bioisoster. Nine novel inhibitors (**13**–**21**) were designed in which a C1- or C2-linked adamantyl or a cubyl group was attached to a 1,2,4-triazole sulfone scaffold (selected for synthetic ease) via either a methylene or ethylene linker (Figure 6.3).

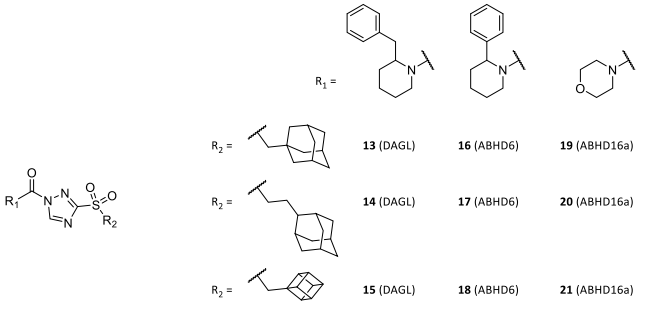


**Figure 6.3. Design of the nine inhibitors synthesized.** Chemical structures of the central sulfonyl triazole urea, the previously developed amines for targeting DAGL, ABHD6 or ABHD16a ($R_1$, indicated at compound number) and the selected caged hydrocarbons ($R_2$).

Synthesis started with commercially available adamantanecarboxylic acid (**22a**) or methyl ester (**22b**) or cubanecarboxylic acid (**22c**), which were reduced to the alcohols **23a**–**c** using $LiAlH_4$ (Scheme 6.1). Subsequent triflation provided a suitable substrate for substitution with potassium thioacetate, affording thioacetates **24a**–**c** in moderate yields (38–64%). Reduction by $LiAlH_4$ and oxidation using molecular bromine afforded the symmetrical disulfides **25a**–**c** (49–99% yield). To synthesize the desired thioether, 1-(pyrrolidin-1-yl-methyl)-1*H*-1,2,4-triazole (synthesized according to literature[58]) was lithiated using *n*-BuLi. Careful addition of disulfide **25a**–**c** led to formation of the thioether, while the pyrrolidin-1-ylmethyl protecting group was removed by the liberated thiol at the same time, providing thioethers **26a**–**c** (65–83% yield). The byproduct originating from the deprotection was easily removed after reduction with $NaBH_4$ in ethanol. The resulting triazole thioether was reacted with the desired carbamoyl chloride, which was either commercially available (4-morpholinecarbonyl chloride) or formed by treating the corresponding piperidine (commercially available 2-benzylpiperidine or 2-phenyl-piperidine **27**) with triphosgene, affording triazole ureas **28a**–**i** (62–73% yield). To obtain the desired sulfone, the thioether was oxidized using peracetic acid, yielding final products **13**–**21** quantitatively. For all inhibitors, an overall yield was achieved of 5 to 29%, which is comparable to or better than previously reported structurally similar inhibitors that do not contain caged hydrocarbon moieties.[53–56,59]

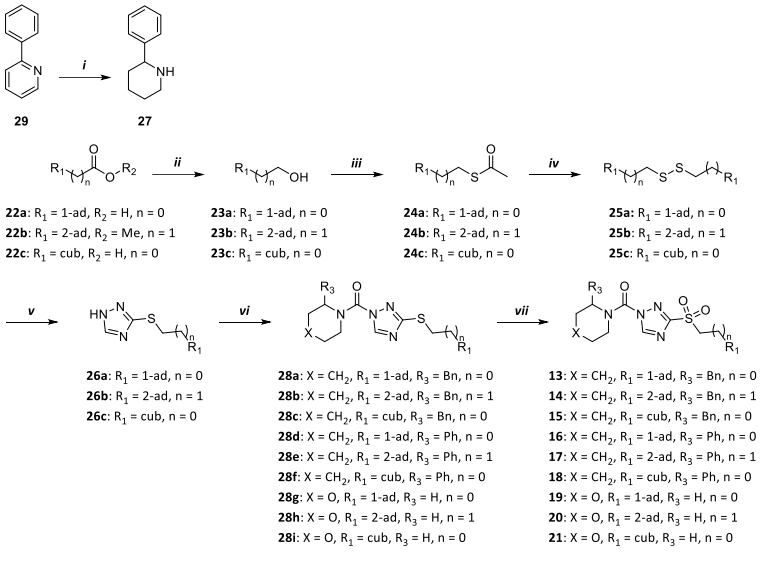


**Scheme 6.1. General synthesis route of diamondoid-containing DAGL, ABHD6 and ABHD16a inhibitors.** Reagents and conditions: *i*) $H_2$, $PtO_2$, HCl, EtOH, 3 h RT; *ii*) $LiAlH_4$, THF, 0.5 h reflux; *iii*) 1. $Tf_2O$, pyr, DCM, 45 min −15°C → RT; 2. AcSK, 18-Crown-6, $CH_3CN$, 72 h RT; *iv*) 1. $LiAlH_4$, THF, 1.5 h RT → 50°C; 2. $Br_2$, DCM/$H_2O$, RT; *v*) 1. 1-(pyrrolydin-1-ylmethyl)-1*H*-1,2,4-triazole, *n*-BuLi, THF, 21 h −80°C → RT; 2. $NaBH_4$, EtOH, 5 min RT; *vi*) 1. 2-benzylpiperidine (**28a**–**c**) or **27** (**28d**–**f**), triphosgene, DIPEA, DCM, 3 h 0°C; 2. 4-morpholinecarbonyl chloride (**28g**–**i**), **26a**–**i**, $K_2CO_3$, DMF, 2–5 d RT; *vii*) AcOOH, DCM, 4–12 h RT. 1-Ad: adamant-1-yl, 2-ad: adamant-2-yl, cub: cubyl.

## Biological evaluation

### Activity of caged hydrocarbon inhibitors in mouse brain proteome

Inhibitors **13**–**21** were tested in mouse brain proteome for their activity against DAGL, ABHD6 or ABHD16a using competitive activity-based protein profiling (cABPP), a powerful chemical biology technique that allows to concomitantly assess inhibitor activity and selectivity in biologically relevant samples.[60,61] In brief, mouse brain membrane proteome was incubated with inhibitor in several concentrations (30 min), followed by broad-spectrum SH probes MB064 or FP-TAMRA, which covalently and fluorescently labeled any residual DAGLα (120 kDa), FAAH (63 kDa), ABHD16a (63 kDa) and ABHD6 (38 kDa) activity. Resolution of the proteins by molecular weight using sodium dodecyl sulfate–polyacrylamide gel electrophoresis (SDS-PAGE) and in-gel fluorescence scanning enabled the determination of the half maximal inhibitory concentration ($IC_{50}$) of the inhibitor for each labeled enzyme. Inhibitors **13**–**21** all inhibited their intended target with $IC_{50}$ values in the sub-micromolar range (Figure 6.4, Table 6.1). Compounds **13**–**15** showed preferential inhibition of DAGLα, with $pIC_{50}$ values between 7.4 and 8.0. It appeared a cubanemethylene moiety yielded the most potent DAGLα inhibitor (**15**), which was also the most selective over ABHD6 (12-fold). **16**–**18** preferentially inhibited ABHD6 ($pIC_{50}$ 6.3–6.8), with 4 to 10-fold selectivity over DAGLα. **17**, bearing a 2-(adamant-2-yl)ethylene moiety, was the most potent ABHD6 inhibitor of this series, as well as the most selective over DAGLα and FAAH ($pIC_{50}$ < 5). **13**–**18** inhibited both ABHD6 and DAGLα at concentrations up to 10 μM, but all but **18** did not inhibit ABHD16a or FAAH. Compounds **19**–**21** did show activity on ABHD16a, with $pIC_{50}$ values between 6.4 and 7.6. However, they had no selectivity over ABHD6 ($pIC_{50}$ 7.3–7.8) and **21** also showed activity on FAAH ($pIC_{50}$ = 5.6). Because of their superior selectivity profile compounds **15** and **17** were selected for further profiling (Supplementary Figure S6.1).

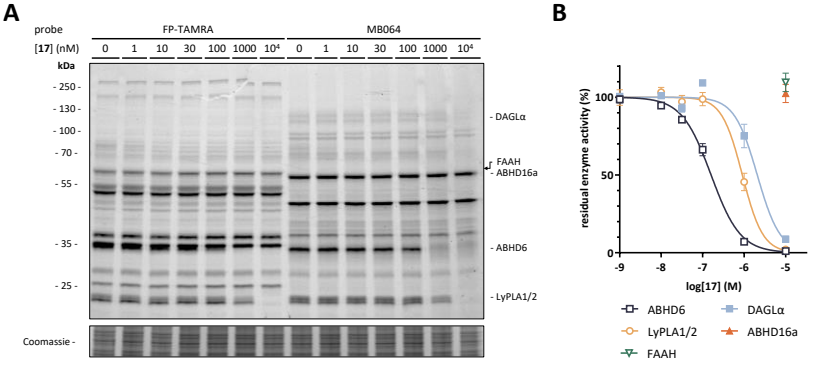


**Figure 6.4. Inhibitory activity of 17 on mouse brain proteome.** A) Representative example gel image of cABPP experiment of **17** on mouse brain proteome. B) Inhibition curves of **17** on mouse brain enzymes as determined by cABPP.

**Table 6.1. *In vitro* activity of 13–21 and reference inhibitors.** $pIC_{50}$ values on ABHD6, ABHD16a, DAGLα and FAAH (left column for each enzyme) determined in cABPP experiments on mouse brain proteome using FP-TAMRA and MB064 (**8**–**10**, **12**–**21**) or on Neuro-2a lysate using FP-TAMRA (**11**). If available, data is presented as mean + SEM (N = 3). The right column states the apparent fold selectivity (app. sel.) of that inhibitor on its intended target (indicated with a "–") over its respective off-targets. NR: data not reported.

| | ABHD6 | | ABHD16a | | DAGLα | | FAAH | |
|---|---|---|---|---|---|---|---|---|
| | $pIC_{50}$ ± SEM | App. sel. | $pIC_{50}$ ± SEM | App. sel. | $pIC_{50}$ ± SEM | App. sel. | $pIC_{50}$ ± SEM | App. sel. |
| **8 ((*R*)-KT109)** | 7.1 ± 0.1[56] | 10 | < 5.0[56] | > 1000 | 8.1 ± 0.1[56] | – | < 5.0[56] | > 1000 |
| **9 (DH376)** | 7.1 ± 0.1[56] | 126 | < 5.0[56] | > 10,000 | 9.2 ± 0.1[56] | – | NR | NR |
| **10 (AJ126)** | 6.1 ± 0.1[54] | 100 | NR | NR | 8.1 ± 0.1[54] | – | NR | NR |
| **13** | 6.49 ± 0.07 | 17 | < 5.0 | > 537 | 7.73 ± 0.08 | – | < 5.0 | > 537 |
| **14** | 7.05 ± 0.03 | 3.4 | < 5.0 | > 380 | 7.58 ± 0.09 | – | < 5.0 | > 380 |
| **15** | 6.84 ± 0.06 | 14 | < 5.0 | > 1000 | 8.00 ± 0.06 | – | < 5.0 | > 1000 |
| **11 (KT182)** | 8.8[53] | – | NR | NR | NR | NR | < 6.0[53] | > 631 |
| **16** | 6.49 ± 0.05 | – | < 5.0 | > 30 | 5.60 ± 0.08 | 7.8 | < 5.0 | > 30 |
| **17 (RED353)** | 6.80 ± 0.03 | – | < 5.0 | > 63 | 5.68 ± 0.07 | 13 | < 5.0 | > 63 |
| **18** | 6.61 ± 0.05 | – | < 5.0 | > 40 | 6.00 ± 0.07 | 4.1 | 5.59 ± 0.06 | 10 |
| **12 (XGN067)** | 8.18 ± 0.08[55] | < 1 | 8.10 ± 0.13[55] | – | 5.46 ± 0.11[55] | 437 | 6.14 ± 0.10[55] | 91 |
| **19** | 7.53 ± 0.05 | < 1 | 7.03 ± 0.07 | – | 5.44 ± 0.19 | 39 | < 5.0 | > 107 |
| **20** | 7.82 ± 0.03 | < 1 | 7.55 ± 0.04 | – | 5.75 ± 0.13 | 63 | < 5.0 | > 354 |
| **21** | 7.26 ± 0.07 | < 1 | 6.36 ± 0.07 | – | 4.91 ± 0.24 | 28 | 5.64 ± 0.04 | 5.2 |

**Profiling of caged hydrocarbon inhibitors as ABHD6 inhibitors in neuronal cells**

The cellular activity of **15** and **17** was investigated in a widely used mouse neuroblastoma cell line (Neuro-2a) that expresses both DAGLβ and ABHD6. In brief, Neuro-2a cells were treated with inhibitor at increasing concentrations (1 h), harvested, lysed and the resulting homogenate was incubated with FP-TAMRA and MB064 to fluorescently label any remaining SH activity. KT182 was taken along for comparison of the results (*in vitro* activity in Supplementary Table S6.1). Both **15** and **17** exhibited a more than 10-fold increased potency at inhibiting ABHD6 ($pIC_{50}$ = 8.1 and 8.4, respectively, Table 6.2) compared to their activity measured in mouse brain lysate (Table 6.1). Their inhibitory activity on other SHs, such as DDHD2, FAAH and LyPLA1 and 2, was also increased (Table 6.2 and Supplementary Table S6.1). Compound **15**'s activity on DAGLβ ($pIC_{50}$ = 6.7) was lower than the activity on DAGLα *in vitro* ($pIC_{50}$ = 8.0), giving it a poor cellular selectivity profile. ABHD6 inhibitor **17** demonstrated an increased selectivity to almost 300-fold over DAGL and 90-fold over LyPLA1/2. Its selectivity over FAAH was more than 60-fold, whereas KT182 showed less than 30-fold selectivity (Table 6.2, Figure 6.5A).

**Table 6.2. Cellular inhibition values of 15, 17 and KT182 on Neuro-2a enzymes.** $pIC_{50}$ values determined from cABPP experiments with probes FP-TAMRA and MB064. Data presented as mean ± SEM (N = 3). For each inhibitor the apparent fold selectivity (app. sel.) on its intended target (indicated with "–")over its respective off-targets is stated in the right column.

| | **15** | | **17** | | **KT182** | |
|---|---|---|---|---|---|---|
| | **$pIC_{50}$ ± SEM** | **App. sel.** | **$pIC_{50}$ ± SEM** | **App. sel.** | **$pIC_{50}$ ± SEM** | **App. sel.** |
| **ABHD6** | 8.10 ± 0.05 | < 1 | 8.39 ± 0.03 | – | 8.87 ± 0.03 | – |
| **ABHD12** | < 5.0 | > 50 | < 5.0 | > 1000 | < 5.0 | > 1000 |
| **ABHD16a** | < 5.0 | > 50 | < 5.0 | > 1000 | < 5.0 | > 1000 |
| **DAGLβ** | 6.74 ± 0.09 | – | 5.92 ± 0.04 | 295 | < 5.0 | > 1000 |
| **DDHD2** | 5.49 ± 0.08 | 18 | < 5.0 | > 1000 | < 5.0 | > 1000 |
| **FAAH** | 6.59 ± 0.09 | 1.4 | 6.58 ± 0.07 | 65 | 7.41 ± 0.06 | 29 |
| **KIAA1363** | < 5.0 | > 50 | < 5.0 | > 1000 | < 5.0 | > 1000 |
| **LyPLA1/2** | 5.88 ± 0.06 | 7.2 | 6.44 ± 0.08 | 89 | 5.99 ± 0.03 | 759 |
| **NTE** | < 5.0 | > 50 | < 5.0 | > 1000 | 6.07 ± 0.15 | 631 |

Since compound **17** showed the most promising ABHD6 inhibitor profile in both cABPP assays, its inhibitory activity was investigated in an orthogonal fluorogenic substrate assay. **17** and KT182 were tested on hABHD6-overexpressing HEK293T cells for their ability to block the hydrolysis of 4-methylumbelliferyl heptanoate (4-MUH). Both **17** and KT182 inhibited the conversion of 4-MUH hydrolysis by ABHD6 with $pIC_{50}$s of 8.8 and 7.9, respectively (Figure 6.5B). Of note, substrate conversion by wild type HEK293T lysate was virtually unaffected even at high concentrations, demonstrating the selectivity of **17**.

Finally, the activity of **17** and KT182 in Neuro-2a was measured with quantifying changes in select lipids using HPLC-MS/MS. Neuro-2a cells were treated with each inhibitor at 100 nM (1 h), a concentration that fully inhibits ABHD6 without affecting DAGLβ, according to the cABPP results (Table 6.2). Although KT182 fully inhibited ABHD6, this treatment did not influence 2-AG levels, whereas **17** substantially lowered these (Figure 6.5C). In addition, KT182 increased AEA levels, whereas **17** did not affect the levels of this second endocannabinoid. These data agree with the recent observation that ABHD6 also possesses DAG lipase activity, thereby contributing to the generation of 2-AG in Neuro-2a cells.[38] The lack of effect on 2-AG levels by KT182 may suggest that FAAH-inhibition and increased NAE-levels indirectly modulate 2-AG biosynthesis. These results show that **17** is a highly potent and one of the most selective inhibitors of ABHD6 identified to date.

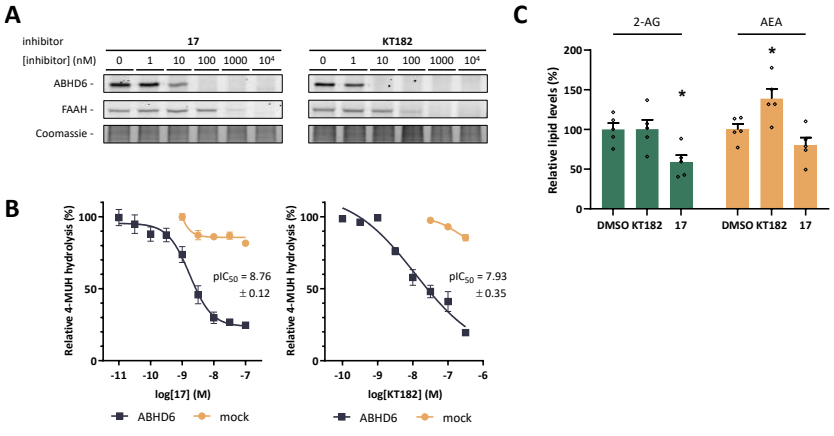


**Figure 6.5. Cellular activity of 17 and KT182.** A) Dose-dependent inhibition of ABHD6 and FAAH in Neuro-2a cells by **17** and KT182. Representative gel image excerpts of cABPP experiments with probes FP-TAMRA and MB064 (full images in Supplementary Figure S6.1). B) Dose-dependent inhibition by **17** and KT182 of 4-MUH hydrolysis on ABHD6-overexpressing or mock HEK293T membrane preparations. Corresponding $pIC_{50}$ values on ABHD6 are indicated. Data presented as mean ± SEM (N ≥ 3). C) Levels of 2-AG (combined with 1-AG) and AEA measured in Neuro-2a by targeted lipidomics analysis after treatment with **17** or KT182 (1h, 100 nM), expressed as relative levels compared to those measured in DMSO-treated cells. Individual measurements are shown, as well as means ± SEM (N = 5). Data were tested for equality by one-way ANOVA with Dunnett's multiple comparison correction. *: adjusted $p < 0.05$.

## Conclusion

In conclusion, caged hydrocarbons were successfully leveraged to develop novel inhibitors of DAGL, ABHD6 and ABHD16a. A bulky 2-(adamant-2-yl)ethylene moiety likely favored the cellular activity of **17** (**RED353**), the most potent and selective ABHD6 inhibitor in this series. This case study shows the first example of caged hydrocarbon structures incorporated in triazole urea-based inhibitors and the first application in lipase inhibitors, providing a new chemical tool for the investigation of the physiological functions of ABHD6. The synthesis and results presented here could expand the medicinal chemists' toolbox with new chemical properties, leading to new possibilities for inhibitor design.

## Acknowledgements

Yevhenii Radchenko is kindly acknowledged for performing organic synthesis and ABPP, Simar Singh and Nephi Stella for 4-MUH assays, Floor Stevens for targeted lipidomics, Hans van den Elst for HRMS analysis. Hans den Dulk is acknowledged for plasmid cloning and purification.

## Experimental procedures

### General remarks

All chemicals and reagents were purchased from Thermo Fisher Scientific or Bio-Rad and used without further purification, unless noted otherwise. Solvents were obtained from Biosolve Chemicals or Merck, salts from Chem-Lab, and used as such. Activity-based probes were purchased from Thermo Fisher Scientific (FP-TAMRA) or synthesized in-house (MB064) (chemical structures in Chapter 3 Supplementary Figure S3.8). Inhibitors were synthesized in-house as described below.

### Cell culture

Neuro-2a (mouse neuroblastoma, ATCC) cells were cultured in DMEM (Sigma-Aldrich, D6546) with additional heat-inactivated new-born calf serum (10% (v/v), Avantor Seradigm), L-Ala-L-Gln (2 mM, Sigma-Aldrich), penicillin and streptomycin (both 200 µg/mL, Duchefa Biochemie) at 37°C, 7% $CO_2$. Medium was refreshed every 2–3 days and cells were passaged twice a week at 70–80% confluence by aspirating the medium, thorough pipetting in fresh medium and seeding to appropriate density. Cell cultures were regularly tested for mycoplasma and discarded after 2–3 months.

### ABHD6 overexpression lysate preparation

HEK293T (human embryonic kidney) cells, seeded to 50% confluence, were transfected with hABHD6 plasmid using polyethyleneimine (PEI, Polysciences). 24 h p.t. medium was aspirated and cells were washed twice with ice-cold PBS. Cells were harvested in ice-cold PBS by scraping or thorough pipetting and centrifuged (4 °C, 1150 × *g*, 10 min). Pellets were flash-frozen in liquid $N_2$ and stored at −80°C until further use.

Cell pellets were thawed on ice and lysed by dounce homogenization in 500 µL TE buffer (50 mM Tris-HCl, 1 mM EDTA, pH 7.4) and subsequent sonication (30 s, 10% amplitude). Protein concentration was determined using Bio-Rad *DC* Protein Assay and aliquots were flash-frozen in liquid $N_2$ and stored at −80°C until further use.

### Mouse brain lysate preparation

Mouse brains were harvested from surplus C57Bl/6J mice (8–14 weeks old) according to guidelines approved by the ethical committee of Leiden University (AVD1060020171144), flash-frozen in liquid $N_2$ and stored at −80°C until use. Upon preparation, intact brains were thawed on ice and homogenized in 6 mL ice-cold lysis buffer (20 mM HEPES, 2 mM DTT, 250 mM sucrose, 1 mM $MgCl_2$, 25 U/mL Benzonase®, pH 6.8) using a Wheaton™ dounce homogenizer (DWK Life Sciences) and incubated on ice for 1 h. Cell debris was removed by low-speed centrifugation (170 × *g*, 5 min, 4°C), after which the supernatant was subjected to ultracentrifugation to separate membrane and cytosol fractions. The pellet was resuspended in ice-cold storage buffer (20 mM HEPES, 2 mM DTT, pH 6.8) and homogenized by passing through an insulin needle. The protein concentrations of both fractions were determined using a Quick Start™ Bradford Protein Assay and samples were diluted to 2.0 mg/mL (membrane) or 1.0 mg/mL (cytosol) using ice-cold storage buffer, aliquoted to single-use volumes, flash-frozen in liquid $N_2$ and stored at −80°C until further use.

### Activity-based protein profiling

Mouse brain lysates were thawed on ice. 19.5 µL lysate was incubated with 0.5 µL inhibitor in DMSO (30 min, RT), followed by 0.5 µL activity-based probe (final concentration 500 nM FP-TAMRA or 250 nM MB064) in DMSO (20 min, RT, final DMSO concentration 5%). The reactions were quenched by

addition of 7 µL 4× Laemmli buffer (240 mM Tris, 8% (w/v) SDS, 40% (v/v) glycerol, 5% (v/v) β-mercaptoethanol (Sigma-Aldrich), 0.04% bromophenol blue). 10 µL sample was resolved on 10% acrylamide SDS-PAGE gel (180 V, 70 min) and afterwards imaged on a Bio-Rad Chemidoc MP using Cy3/TAMRA settings (ex. 532/12 nm, em. 602/50 nm). Coomassie Brilliant Blue R250 staining was used for total protein loading correction. Images were analyzed using Bio-Rad Image Lab 6. $IC_{50}$ calculations were performed in GraphPad Prism 7.

## ABPP of *in situ* treatments

Two days prior to treatment, Neuro-2a cells were seeded to 12-wells plates (~$0.25 \cdot 10^6$ cells per well). Before the experiment was started medium was aspirated. Medium with DMSO or inhibitor in DMSO (0.25% (v/v) DMSO) was added and cells were incubated for 1 h at 37°C. Then medium was aspirated and cells were washed with RT Dulbecco's PBS (Sigma-Aldrich). Cells were harvested in ice-cold PBS by thorough pipetting and centrifuged (1000 × *g*, 6 min, RT). Pellets were flash-frozen in liquid $N_2$ and stored at −80°C until further use.

Cell pellets were thawed on ice and lysed in 50 µL lysis buffer. After incubation on ice for 1 h, the protein concentration was determined using Quick Start™ Bradford Protein Assay and the samples were diluted to 1.0 or 2.0 mg/mL using storage buffer. 19.5 µL of this whole lysate was incubated with 0.5 µL FP-TAMRA (500 nM) or MB064 (2 µM) in DMSO (20 min, RT). Reactions were then quenched, proteins resolved and images analyzed as described under Activity-based protein profiling.

## Biochemical fluorogenic substrate assay

Lysate was thawed on ice and diluted to 0.024 mg/mL in TE buffer. To each well of a Greiner Bio-One black 96-wells plate with clear, flat bottom, 10 µL inhibitor (or DMSO) solution in TE buffer was added. After short vortex, 85 µL lysate (2 µg total protein) was added and the plate was incubated for 30 min at 37°C. 5 µL 1 mM 4-methylumbelliferyl heptanoate in EtOH was added (final concentration 50 µM) and fluorescence was measured immediately every 1–2 minutes for 120 min (ex. 355 nm, em. 460 nm, 37 °C). $IC_{50}$ calculations were performed in GraphPad Prism 7.

## Targeted lipidomics

### Sample preparation

One or two days prior to treatment, Neuro-2a cells were seeded to 6 cm dishes (~$2.5 \cdot 10^6$ cells per dish). Before the experiment was started medium was aspirated and cells were washed with RT PBS. Treatment medium with DMSO or inhibitor in DMSO (0.25% (v/v) DMSO) was added and cells were incubated for 1 h at 37°C. Then medium was removed and cells were washed with RT PBS. Cells were harvested in 1250 µL RT PBS by thorough pipetting. 1000 µL was centrifuged (1000 × *g*, 6 min, RT) in Eppendorf® Safe-Lock tubes. Cell count was performed on the remaining 250 µL, after which this was centrifuged as well. Pellets were flash-frozen in liquid $N_2$ and stored at −80°C until further use.

The 250-µL pellets were thawed on ice and lysed in 50 µL lysis buffer. After incubation on ice for 30 min, the protein concentration was determined using Quick Start™ Bradford Protein Assay.

### Lipid extraction

Pellets were thawed on ice. To each 1000-µL pellet, 10 µL internal standard mix (deuterated reference lipids 2-arachidonoyl glycerol-$d_8$, *N*-arachidonoyl ethanolamine-$d_8$, *N*-docosahexaenoyl ethanolamine-$d_4$, *N*-linoleoyl ethanolamine-$d_4$, *N*-oleoyl ethanolamine-$d_4$, *N*-palmitoyl ethanolamine-$d_5$, *N*-stearoyl ethanolamine-$d_3$, *N*-eicosapentaenoyl ethanolamine-$d_4$ and arachidonic acid-$d_8$, Cayman Chemical Company) was added, followed by 100 µL extraction buffer (100 mM $NH_4OAc$, 0.5% (m/v) NaCl, pH 4). After short mixing, 1000 µL MTBE was added and lipids were

extracted in a Next Advance Bullet Blender® Blue tissue homogenizer (7 min, 80% speed, RT) followed by centrifugation (16,000 × *g*, 11 min, 4°C). 925 µL of the organic layer was transferred into clean, pre-cooled tubes and concentrated in an Eppendorf® Concentrator Plus (40 min, 30°C). The lipid residue was reconstituted in 30 µL 9:1 (v/v) $CH_3CN$:$H_2O$ by thorough mixing, centrifuged (10,000 × *g*, 4 min, 4°C) and 25 µL was transferred to LC-MS vials (KG 09 0188, Screening Devices) with insert (ME 06 0232, Screening Devices).

**LC-MS/MS analysis**

10 µL of sample was injected into the system, consisting of an Acquity UPLC I class binary solvent manager pump in conjugation with a tandem quadrupole mass spectrometer (Waters Corporation). The separation was performed in an Acquity HSS T3 column (2.1 × 100 mm, 1.8 µm) maintained at 45°C, with the eluent flow rate set to 0.55 mL/min. The mobile phase consisted of 2 mM $NH_4HCO_2$, 10 mM formic acid in water (A) and $CH_3CN$ (B). Initial gradient conditions were 55% B for 0.5 min, then linearly increased to 60% over 1.5 min. The gradient was then linearly ramped up to 100% B over 5 min and then held for 2 min. After 10 s the system returned to the initial conditions, which were held for 2 min before the next injection. For lipid quantification ESI-MS and a selective multiple reaction mode (sMRM) were used, with individually optimized MRM transitions for target compounds using synthetic standards and internal standards (see Lipid extraction protocol for composition). Peak area integration was performed manually with MassLynx 4.1 (Waters Corporation). Absolute values of lipid levels were calculated by correction for internal standard peak area and comparison to the calibration curve of the respective synthetic standard. In case of 2-AG, combined levels of 1-AG and 2-AG were calculated and compared to combined internal standard.

Lipid levels were corrected for cell count or protein concentration. Statistical analysis was performed using GraphPad Prism 8. For each lipid, one-way ANOVA was performed between treatment and control groups, with Dunnett's multiple comparison correction for using one control group for both treatment groups.

## Organic synthesis

**General remarks**

All reagents were purchased from Sigma-Aldrich, Acros Organics, Merck or Fluorochem and used without further purification. Solvents were purchased from Sigma-Aldrich, VWR Chemicals, Honeywell Riedel-de Haën or Biosolve Chemicals, common salts from Sigma-Aldrich or Chem-Lab, and used without further purification. Moisture-sensitive reactions were carried out in solvents dried over heat-activated molecular sieves (4 Å, Sigma-Aldrich), using flame-dried glassware under an atmosphere of $N_2$. TLC analysis was performed on Merck silica gel 60 $F_{254}$ aluminum TLC plates, on which compounds were visualized under 254 or 366 nm UV light and using $KMnO_4$ (30 mM $KMnO_4$, 180 mM $K_2CO_3$ in water) or ninhydrin (7.5 mM ninhydrin, 10% (v/v) AcOH in EtOH) stain. Flash column chromatography was performed using $SiO_2$ (Macherey-Nagel, 60 M) as stationary phase.

NMR spectra were recorded on a Bruker AV-400 MHz or AV-500 MHz spectrometer at 400 MHz ($^1$H) and 101 MHz ($^{13}$C) or 500 MHz ($^1$H) and 126 MHz ($^{13}$C) respectively, using $CDCl_3$ (Eurisotop) as solvent. Chemical shifts are reported in ppm with TMS ($^1$H, δ 0.00) or solvent resonance ($^{13}$C, δ 77.16) as internal standard. Data are reported as follows: chemical shift δ (ppm), multiplicity (s = singlet, d = doublet, t = triplet, p = pentet, dd = doublet of doublets, td = triplet of doublets, qd = quartet of doublets, dt = doublet of triplets, bs = broad singlet ($^1$H), br = broad ($^{13}$C), m = multiplet), coupling constants *J* (Hz) and integration. HPLC-MS analysis was performed on a Finnigan Surveyor HPLC system equipped with a Macherey-Nagel NUCLEODUR $C_{18}$ Gravity, 5 µm, 50×4.6 mm column followed

by a Thermo Scientific LTQ Orbitrap XL spectrometer, using $H_2O/CH_3CN$ + 1% TFA as mobile phase. All compounds used for biological experiments were ≥95% pure based on LC-MS UV absorbance.

**General procedure A**

Peracetic acid (10–15 eq, 36–40% in AcOH) was added to a solution of triazole urea thioether (1 eq) in DCM (150 mL/mmol) and the mixture was stirred for 4–12h. Upon completion the reaction mixture was diluted with DCM, washed with water and brine and concentrated *in vacuo*. Flash column chromatography yielded the sulfone final product.

**General procedure B**

A solution of adamantanecarboxylic acid or ester (1 eq) in dry THF (10 mL/g) was added dropwise to an ice-cold suspension of $LiALH_4$ (2.5 eq) in dry THF (20 mL/g). The reaction mixture was warmed to RT and stirred for 30 min, followed by reflux for 30 min. The reaction was then quenched by addition of 10% aq. NaOH on an ice bath. Solids were removed by filtration and washed with DCM. Combined filtrates were dried over $Na_2SO_4$, filtrated and concentrated *in vacuo*. The product was used without further purification.

**General procedure C**

Triflic anhydride (1.05 eq) was added portionwise to a solution of alcohol (1 eq) and pyridine (1.2 eq) in dry DCM (15 mL/g), while maintaining the temperature between −15 and −5°C. The mixture was stirred for 15 min followed by 30 min at RT. The mixture was then diluted with hexane (30 mL/g), cooled to 0°C and ice-cold 1 M aq. $H_2SO_4$ was added until pH < 7. The layers were separated, the organic layer was washed with water and brine, dried over $Na_2SO_4$, filtrated and concentrated *in vacuo*. The resulting brown liquid was dissolved in $CH_3CN$ (10 mL/g) and cooled to 0°C. AcSK (2 eq) and 18-Crown-6 (0.3 eq) were added, the mixture was warmed to RT and stirred for ≥72 h. Solids were removed by filtration and washed with hexane until they were colorless. Combined filtrates were concentrated *in vacuo*. Flash column chromatography (150:1 hexane:EtOAc) provided the thioacetate.

**General procedure D**

To an ice-cold solution of $LiAlH_4$ (1.5 eq) in dry THF (20 mL/g), a solution of thioacetate (1 eq) in dry THF (10 mL/g) was added dropwise. The reaction mixture was allowed to warm to RT and stirred for 30 min, followed by 1 h at 50°C. The reaction was cooled and quenched by addition of 0.1 M aq. HCl on an ice bath. Solids were removed by filtration and washed with DCM. Combined filtrates were concentrated *in vacuo*. The resulting yellow oil was dissolved in DCM (20 mL/g) and added to a suspension of silica powder (5 g/g) in water (2.5 mL/g). 1 M $Br_2$ in DCM was added until the mixture started to color. Solids were removed by filtration. The filtrate was dried over $Na_2SO_4$, filtrated and concentrated *in vacuo*. Silica plug purification with pentane provided the disulfide.

**General procedure E**

A solution of 1-(pyrrolidin-1-ylmethyl)-1*H*-1,2,4-triazole (2 eq)[58] in dry THF (10 mL/mmol) was degassed by $N_2$ purging and cooled to −80°C. *n*-BuLi (2.3 M in THF, 2.2 eq) was added portionwise, after which the reaction mixture was stirred at −80°C for 30 min followed by 90 min at −30 to −25°C during which a white precipitate formed. The mixture was then cooled to −80°C and a solution of disulfide (1 eq) in dry THF (3 mL/mmol) was added portionwise. The reaction was stirred for ≥3 h at −75°C, after which it was allowed to warm to RT and stirred overnight. Volatiles were removed under reduced pressure, after which the concentrate was diluted in DCM and washed with water. The organic layer was concentrated *in vacuo*. The residue was brought onto a silica gel column and washed with

pentane and DCM. The product was then eluted using 1:1 DCM:MeOH. The fractions containing product were combined and concentrated *in vacuo*.

The product was treated with $NaBH_4$ in EtOH (20 eq, 20 mL/mmol) and stirred for 5 min. Volatiles were removed under reduced pressure, after which the residue was dissolved in DCM and washed with water and brine. The organic layer was concentrated *in vacuo*. The residue was dispersed in 5 M aq. KOH and extracted with $CHCl_3$. The pH of the aqueous layer was lowered to 7, after which it was again extracted with $CHCl_3$. The combined organic layers were dried over $Na_2SO_4$, filtrated and concentrated *in vacuo* yielding the triazole thioether, which was used without further purification.

**General procedure F**

To an ice-cold solution of triphosgene (1 eq) dry DCM (25 mL/mmol), 2-phenylpiperidine or 2-benzylpiperidine (1 eq) and DIPEA (3 eq) were added. The mixture was stirred on ice for 90 min. When TLC analysis confirmed full conversion the mixture was diluted with DCM and washed with 1 M aq. HCl and brine, dried over $Na_2SO_4$, filtrated and concentrated *in vacuo*. Water was removed by co-evaporation with toluene. The resulting oil was dissolved in dry DMF (150 mL/mmol), triazole thioether (1 eq) and $K_2CO_3$ (3 eq) were added and the reaction mixture was stirred for 2–5 days. The mixture was diluted with DCM, washed with water and brine, dried over $Na_2SO_4$, filtrated and concentrated *in vacuo*. Flash column chromatography afforded the triazole urea thioether.

**General procedure G**

4-Morpholinecarbonyl chloride (2 eq), $K_2CO_3$ (3.5 eq) and triazole thioether (1 eq) were dissolved in dry DMF (175 mL/mmol) and stirred for 48 h. The mixture was then concentrated in vacuo and dissolved in DCM, washed with water and brine, dried over $Na_2SO_4$, filtrated and concentrated in vacuo. Flash column chromatography afforded the triazole urea thioether.

**(3-(((Adamant-1-yl)methyl)sulfonyl)-1*H*-1,2,4-triazol-1-yl)(2-benzylpiperidin-1-yl)methanone (13)**

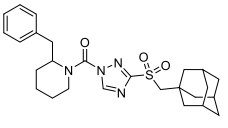

**28a** (13 mg, 0.029 mmol) was oxidized according to General procedure A to obtain the title compound as a white solid (14 mg, 0.029 mmol, quant.).
$^1$H NMR (500 MHz, $CDCl_3$) δ 7.87 (bs, 1H), 7.35 – 6.94 (m, 5H), 4.81 – 4.71 (m, 1H), 4.33 – 4.18 (m, 1H), 3.41 – 3.26 (m, 1H), 3.26 – 3.12 (m, 3H), 2.81 – 2.60 (m, 1H), 1.99 (p, *J* = 3.1 Hz, 3H), 1.96 – 1.57 (m, 18H).
$^{13}$C NMR (126 MHz, $CDCl_3$) δ 162.88, 147.20, 137.70, 129.16, 128.98, 127.07, 66.26, 56.87, 41.99, 41.26, 36.70, 36.42, 34.71, 28.73, 28.39, 25.30, 18.83.
HRMS: $[M+Na]^+$ calculated for $C_{26}H_{34}N_4NaO_3S$ 505.22438, found 505.22396.

**(3-(((Adamant-2-yl)ethyl)sulfonyl)-1*H*-1,2,4-triazol-1-yl)(2-benzylpiperidin-1-yl)methanone (14)**

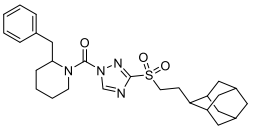

**28b** (8 mg, 0.02 mmol) was oxidized according to General procedure A to obtain the title compound as a white solid (12 mg, 0.025 mmol, quant.).
$^1$H NMR (500 MHz, $CDCl_3$) δ 7.89 (bs, 1H), 7.27 – 6.94 (m, 5H), 4.87 – 4.73 (m, 1H), 4.33 – 4.20 (m, 1H), 3.42 – 3.27 (m, 3H), 3.26 – 3.12 (m, 1H), 2.74 – 2.63 (m, 1H), 2.04 – 1.48 (m, 23H).
$^{13}$C NMR (126 MHz, $CDCl_3$) δ 161.24, 147.48, 137.69, 129.12, 128.99, 127.10, 56.87, 53.15, 43.48, 41.29, 38.96, 38.18, 36.73, 31.61, 31.40, 28.77, 28.09, 27.88, 25.33, 24.77, 18.84.
HRMS: $[M+Na]^+$ calculated for $C_{27}H_{36}N_4NaO_3S$ 519.24003, found 519.23964.

**(2-Benzylpiperidin-1-yl)(3-((cuban-1-ylmethyl)sulfonyl)-1*H*-1,2,4-triazol-1-yl)methanone (15)**

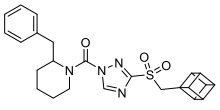

**28c** (10 mg, 0.024 mmol) was oxidized according to General procedure A to obtain the title compound as a white solid (13 mg, 0.029 mmol, quant.).
$^1$H NMR (500 MHz, $CDCl_3$) δ 7.93 (bs, 1H), 7.27 – 6.93 (m, 5H), 4.83 – 4.73 (m, 1H), 4.34 – 4.21 (m, 1H), 3.99 – 3.94 (m, 1H), 3.94 – 3.88 (m, 6H), 3.73 (s, 2H), 3.40 – 3.26 (m, 1H), 3.26 – 3.14 (m, 1H), 2.78 – 2.64 (m, 1H), 2.03 – 1.52 (m, 7H).
$^{13}$C NMR (126 MHz, $CDCl_3$) δ 162.14, 147.47, 137.67, 129.19, 128.98, 127.10, 57.56, 56.84, 49.30, 48.11, 45.03, 41.29, 36.68, 28.76, 25.42, 18.82.
HRMS: $[M+Na]^+$ calculated for $C_{24}H_{26}N_4O_3S$ 473.16178, found 473.16153.

**(3-(((Adamant-1-yl)methyl)sulfonyl)-1*H*-1,2,4-triazol-1-yl)(2-phenylpiperidin-1-yl)-methanone (16)**

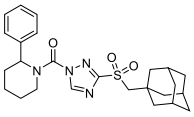

**28d** (12 mg, 0.027 mmol) was oxidized according to General procedure A to obtain the title compound as a white solid (11 mg, 0.023 mmol, 85%).
$^1$H NMR (500 MHz, $CDCl_3$) δ 8.88 (s, 1H), 7.44 – 7.36 (m, 2H), 7.34 – 7.27 (m, 3H), 5.83 – 5.77 (m, 1H), 4.32 – 4.25 (m, 1H), 3.21 (s, 2H), 3.15 (td, *J* = 13.7, 3.1 Hz, 1H), 2.54 – 2.44 (m, 1H), 2.15 – 2.05 (m, 1H), 1.97 (p, *J* = 3.1 Hz, 3H), 1.87 – 1.61 (m, 16H).
$^{13}$C NMR (126 MHz, $CDCl_3$) δ 163.57, 148.67, 148.15, 137.73, 129.18, 127.53, 126.59, 66.18, 56.67 (br), 43.71 (br), 42.01, 36.44, 28.42, 28.02, 25.63, 19.23.
HRMS: $[M+Na]^+$ calculated for $C_{25}H_{32}N_4NaO_3S$ 491.20873, found 491.20830.

**(3-((2-(Adamant-2-yl)ethyl)sulfonyl)-1*H*-1,2,4-triazol-1-yl)(2-phenylpiperidin-1-yl)methanone (17, RED353)**

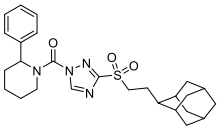

**28e** (12 mg, 0.027 mmol) was oxidized according to General procedure A to obtain the title compound as a white solid (9 mg, 0.02 mmol, 70%).
$^1$H NMR (500 MHz, $CDCl_3$) δ 8.91 (s, 1H), 7.42 – 7.37 (m, 2H), 7.34 – 7.28 (m, 3H), 5.83 – 5.77 (m, 1H), 4.33 – 4.25 (m, 1H), 3.40 – 3.27 (m, 2H), 3.20 – 3.10 (m, 1H), 2.53 – 2.45 (m, 1H), 2.15 – 2.05 (m, 1H), 2.00 – 1.92 (m, 2H), 1.91 – 1.61 (m, 17H), 1.55 – 1.47 (m, 2H).
$^{13}$C NMR (126 MHz, $CDCl_3$) δ 162.08, 148.59, 148.34, 137.67, 129.18, 127.54, 126.58, 56.70 (br), 53.06, 43.73 (br), 43.47, 38.99, 38.21, 31.61, 31.42, 28.12, 27.99, 27.90, 25.66, 24.70, 19.22.
HRMS: $[M+Na]^+$ calculated for $C_{26}H_{34}N_4O_3S$ 505.22438, found 505.22407.

**(2-Phenylpiperidin-1-yl)(3-((cuban-1-ylmethyl)sulfonyl)-1*H*-1,2,4-triazol-1-yl)methanone (18)**

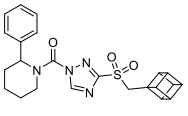

**28f** (16 mg, 0.030 mmol) was oxidized according to General procedure A to obtain the title compound as a white solid (8 mg, 0.017 mmol, 58%).
$^1$H NMR (500 MHz, $CDCl_3$) δ 8.90 (s, 1H), 7.43 – 7.37 (m, 2H), 7.33 – 7.27 (m, 3H), 5.85 – 5.76 (m, 1H), 4.33 – 4.25 (m, 1H), 4.00 – 3.95 (m, 1H), 3.94 – 3.89 (m, 6H), 3.73 (s, 2H), 3.16 (td, *J* = 13.9, 3.4 Hz, 1H), 2.54 – 2.45 (m, 1H), 2.15 – 2.05 (m, 1H), 1.88 – 1.64 (m, 4H).
$^{13}$C NMR (126 MHz, $CDCl_3$) δ 162.80, 148.59, 148.33, 137.73, 129.18, 127.54, 126.58, 57.45, 56.65 (br), 51.12, 49.37, 48.15, 45.06, 43.80 (br), 28.03, 25.66, 19.23.
HRMS: $[M+Na]^+$ calculated for $C_{23}H_{24}N_4O_3S$ 459.14613, found 459.14559.

**(3-(((Adamant-1-yl)methyl)sulfonyl)-1*H*-1,2,4-triazol-1-yl)(morpholino)methanone (19)**

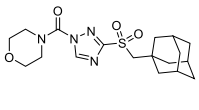

**28g** (5 mg, 0.01 mmol) was oxidized according to General procedure A to obtain the title compound as a white solid (5 mg, 0.01 mmol, 92%).
*Analytical data on next page.*

$^1$H NMR (500 MHz, $CDCl_3$) δ 8.88 (s, 1H), 4.10 – 3.64 (m, 8H), 3.25 (s, 2H), 2.03 – 1.96 (m, 3H), 1.87 – 1.81 (m, 6H), 1.77 – 1.64 (m, 6H).
$^{13}$C NMR (126 MHz, $CDCl_3$) δ 163.76, 148.33, 147.35, 66.58, 66.25, 48.19 (br), 45.97 (br), 42.07, 36.44, 28.43.
HRMS: $[M+Na]^+$ calculated for $C_{18}H_{26}N_4NaO_4S$ 417.15670, found 417.15615.

**(3-((2-(Adamant-2-yl)ethyl)sulfonyl)-1*H*-1,2,4-triazol-1-yl)(morpholino)methanone (20)**

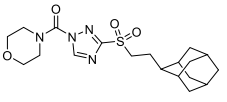

**28h** (9 mg, 0.02 mmol) was oxidized according to General procedure A to obtain the title compound as a white solid (9 mg, 0.02 mmol, 92%).
$^1$H NMR (500 MHz, $CDCl_3$) δ 8.91 (s, 1H), 4.14 – 3.61 (m, 8H), 3.44 – 3.35 (m, 2H), 2.01 – 1.94 (m, 2H), 1.92 – 1.66 (m, 13H), 1.56 – 1.49 (m, 2H).
$^{13}$C NMR (126 MHz, $CDCl_3$) δ 162.27, 148.51, 147.26, 66.56, 53.10, 48.08 (br), 45.97 (br), 43.50, 38.98, 38.19, 31.63, 31.43, 28.10, 27.90, 24.73.

**(3-((Cuban-1-ylmethyl)sulfonyl)-1*H*-1,2,4-triazol-1-yl)(morpholino)methanone (21)**

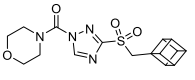

**28i** (13 mg, 0.038 mmol) was oxidized according to General procedure A to obtain the title compound as a white solid (13 mg, 0.034 mmol, 91%).
$^1$H NMR (500 MHz, $CDCl_3$) δ 8.91 (s, 1H), 4.02 – 3.96 (m, 2H), 3.95 – 3.91 (m, 8H), 3.90 – 3.71 (m, 4H), 3.77 (s, 3H).
$^{13}$C NMR (126 MHz, $CDCl_3$) δ 162.99, 148.46, 147.23, 66.56, 57.49, 49.35, 48.15, 46.02 (br), 45.06.
HRMS: $[M+Na]^+$ calculated for $C_{16}H_{18}N_4O_4S$ 385.09410, found 385.09299.

**1-Adamantanemethanol (23a)**

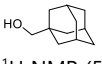

1-Adamantanecarboxylic acid **22a** (5.0 g, 28 mmol) was reduced according to General procedure B to obtain the title compound as a white solid (4.7 g, 27 mmol, 99%).
$^1$H NMR (500 MHz, $CDCl_3$) δ 3.20 (s, 2H), 2.00 (p, *J* = 3.1 Hz, 3H), 1.77 – 1.61 (m, 7H), 1.51 (d, *J* = 2.9 Hz, 6H).
$^{13}$C NMR (126 MHz, $CDCl_3$) δ 77.41, 77.16, 76.91, 74.03, 39.17, 37.31, 34.62, 28.31.

**2-Adamantaneethanol (23b)**

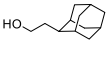

Methyl 2-(adamant-2-yl)acetate **22b** (32.0 g, 154 mmol)[64] was reduced according to General procedure B to obtain the title compound as a white solid (27.0 g, 150 mmol, 97%) which was used without characterization.

***S*-(adamant-1-ylmethyl)thioacetate (24a)**

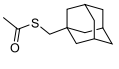

**23a** (5.0 g, 30 mmol) was treated according to General procedure C to obtain the title compound as a red solid (4.3 g, 19 mmol, 64%).
$^1$H NMR (500 MHz, $CDCl_3$) δ 2.73 (s, 2H), 2.35 (s, 3H), 1.96 (p, *J* = 3.0 Hz, 3H), 1.72 – 1.54 (m, 10H), 1.50 (d, *J* = 2.9 Hz, 6H).
$^{13}$C NMR (126 MHz, $CDCl_3$) δ 196.16, 42.62, 41.56, 36.88, 33.37, 30.89, 28.57.

***S*-(2-(adamant-2-yl)ethyl)thioacetate (24b)**

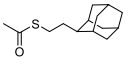

**23b** (3.0 g, 17 mmol) was treated according to General procedure C (with the exception that in the first step the mixture was stirred at −70°C instead of −15 to −5°C) to obtain the title compound as a red liquid (2.2 g, 9.2 mmol, 56%).
$^1$H NMR (400 MHz, $CDCl_3$) δ 2.89 – 2.81 (m, 2H), 2.32 (s, 3H), 1.92 – 1.64 (m, 11H), 1.57 – 1.47 (m, 3H).
$^{13}$C NMR (101 MHz, $CDCl_3$) δ 195.91, 43.80, 39.07, 38.30, 32.43, 31.60, 31.57, 28.21, 27.98, 27.57.

**_S_-(cuban-1-ylmethyl)thioacetate (24c)**

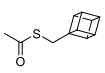

DIAD (2 eq, 2.28 mL, 11.6 mmol) was added dropwise to a solution of $PPh_3$ (2 eq. 3.05 g, 11.6 mmol) in dry THF (15 mL) while keeping the temperature between −5°C and 0°C. The mixture was warmed to RT, stirred for 15 min and cooled back to −5°C. To this, a solution of (cuban-1-yl)methanol (1 eq, 780 mg, 5.81 mmol)[30] and thioacetic acid (2 eq, 820 µL, 11.6 mmol) in dry THF (15 mL) was added dropwise while keeping the temperature below 0°C. The reaction mixture was stirred for 1 h at 0°C followed by 30 min at RT, resulting in a yellow solution. This was poured into 90 mL of 10:1 hexane:EtOAc and concentrated under reduced pressure to 25 mL. Solids were removed by filtration and the filtrate was concentrated *in vacuo*. Flash column chromatography (150:1 hexane:EtOAc) afforded the title compound as a brown oil with an intense odor (420 mg, 2.18 mmol, 38%).

$^1$H NMR (500 MHz, $CDCl_3$) δ 4.04 – 3.98 (m, 1H), 3.88 – 3.82 (m, 3H), 3.78 – 3.72 (m, 3H), 3.20 (s, 2H), 2.36 (s, 3H).

$^{13}$C NMR (126 MHz, $CDCl_3$) δ 196.13, 56.67, 48.84, 48.55, 43.94, 32.54, 30.85.

**Bis(adamant-1-ylmethyl)disulfide (25a)**

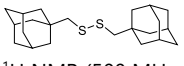

**24a** (1.0 g, 4.5 mmol) was treated according to General procedure D to obtain the title compound as a white solid (790 g, 2.18 mmol, 98%).

$^1$H NMR (500 MHz, $CDCl_3$) δ 2.63 (s, 4H), 1.98 (p, *J* = 3.1 Hz, 6H), 1.73 – 1.59 (m, 12H), 1.57 (d, *J* = 2.9 Hz, 12H).

$^{13}$C NMR (126 MHz, $CDCl_3$) δ 56.23, 41.90, 36.97, 34.33, 28.61.

**Bis(2-(adamant-2-yl)ethyl)disulfide (25b)**

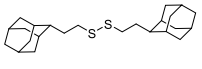

**24b** (1.05 g, 4.40 mmol) was treated according to General procedure D to obtain the title compound as a white crystalline solid (430 g, 1.10 mmol, 50%).

$^1$H NMR (400 MHz, $CDCl_3$) δ 2.73 – 2.65 (m, 4H), 1.92 – 1.66 (m, 30H), 1.52 (d, *J* = 12.6 Hz, 4H).

$^{13}$C NMR (101 MHz, $CDCl_3$) δ 77.48, 77.16, 76.84, 43.58, 39.24, 38.46, 37.68, 32.47, 31.86, 31.79, 28.37, 28.16.

**Bis(cuban-1-ylmethyl)disulfide (25c)**

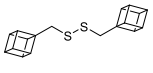

**24c** (420 mg, 2.18 mmol) was treated according to General procedure D to obtain the title compound as a white solid (0.16 g, 0.54 mmol, 49%).

$^1$H NMR (500 MHz, $CDCl_3$) δ 4.08 – 3.99 (m, 2H), 3.95 – 3.85 (m, 12H), 3.05 (s, 4H).

$^{13}$C NMR (126 MHz, $CDCl_3$) δ 77.41, 77.16, 76.91, 57.47, 48.96, 48.72, 44.34, 43.81, 30.46.

**3-(((Adamant-1-yl)methyl)thio)-1*H*-1,2,4-triazole (26a)**

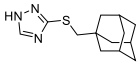

**25a** (405 mg, 1.12 mmol) was treated according to General procedure E to obtain the title compound as a white solid (89 mg, 0.36 mmol, 65%).

$^1$H NMR (400 MHz, $CDCl_3$) δ 10.80 (bs, 1H), 8.15 (s, 1H), 3.08 (s, 1H), 2.01 – 1.95 (m, 4H), 1.74 – 1.53 (m, 11H).

$^{13}$C NMR (101 MHz, $CDCl_3$) δ 157.87, 148.01, 46.99, 41.54, 36.78, 33.89, 28.51.

**3-((2-(Adamant-2-yl)ethyl)thio)-1*H*-1,2,4-triazole (26b)**

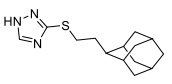

**25b** (393 mg, 1.01 mmol) was treated according to General procedure E to obtain the title compound as a white solid (220 mg, 0.835 mmol, 83%).

$^1$H NMR (500 MHz, $CDCl_3$) δ 8.15 (s, 1H), 3.21 – 3.14 (m, 2H), 1.90 – 1.75 (m, 9H), 1.75 – 1.68 (m, 6H), 1.54 – 1.47 (m, 2H).

$^{13}$C NMR (126 MHz, $CDCl_3$) δ 157.19, 148.10, 43.73, 39.16, 38.40, 32.62, 31.76, 31.72, 31.42, 28.30, 28.09, 0.13.

**3-((Cuban-1-ylmethyl)thio)-1*H*-1,2,4-triazole (26c)**

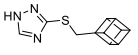

**25c** (150 mg, 0.503 mmol) was treated according to General procedure E to obtain the title compound as a white solid (75 mg, 0.35 mmol, 69%).

$^1$H NMR (500 MHz, $CDCl_3$) δ 12.60 (bs, 1H), 8.15 (s, 1H), 4.02 – 3.96 (m, 1H), 3.90 – 3.81 (m, 3H), 3.81 – 3.74 (m, 3H), 3.52 (s, 2H).

$^{13}$C NMR (126 MHz, $CDCl_3$) δ 148.23, 57.14, 48.71, 48.62, 44.09, 36.64.

**2-Phenylpiperidine (27)**

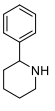

2-Phenylpyridine **29** (1.0 g, 6.4 mmol) was dissolved in EtOH (25 mL) and degassed by $N_2$ purging with a balloon. 1 mL 12 M HCl and $PtO_2$ (8 mol%, 117 mg, 0.515 mmol) were added and the mixture was stirred for 3 h under continuous $H_2$ purging with a balloon. The reaction was quenched by $N_2$ purging with a balloon, after which the catalyst was removed by filtration over celite. The filtrate was concentrated *in vacuo*. Flash column chromatography (7:3 EtOAc:10% $NH_4OH$ in MeOH) afforded the title compound as a yellow oil (85 mg, 0.53 mmol, 7.9%).

$^1$H NMR (500 MHz, $CDCl_3$) δ 7.39 – 7.34 (m, 2H), 7.34 – 7.28 (m, 2H), 7.26 – 7.21 (m, 1H), 3.59 (dd, *J* = 10.6, 2.6 Hz, 1H), 3.24 – 3.16 (m, 1H), 2.80 (td, *J* = 11.6, 2.8 Hz, 1H), 1.92 – 1.85 (m, 1H), 1.83 – 1.73 (m, 1H), 1.71 – 1.62 (m, 1H), 1.62 – 1.42 (m, 3H).

$^{13}$C NMR (126 MHz, $CDCl_3$) δ 145.56, 128.50, 127.17, 126.78, 62.47, 47.91, 35.03, 26.47, 25.97, 25.55.

**(3-(((Adamant-1-yl)methyl)thio)-1*H*-1,2,4-triazol-1-yl)(2-benzylpiperidin-1-yl)methanone (28a)**

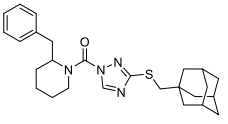

2-Benzylpiperidine (1.5 eq, 11 mg, 0.060 mmol) and **26a** (1 eq, 10 mg, 0.040 mmol) were coupled according to General procedure F to obtain the title compound as a white solid (13 mg, 0.029 mmol, 73%).

$^1$H NMR (500 MHz, $CDCl_3$) δ 8.05 (bs, 1H), 7.27 – 7.17 (m, 3H), 7.11 – 7.05 (m, 2H), 5.01 – 4.79 (m, 1H), 4.39 – 4.18 (m, 1H), 3.24 (td, *J* = 13.3, 2.8 Hz, 1H), 3.19 – 3.11 (m, 1H), 3.09 – 2.96 (m, 2H), 2.91 – 2.67 (m, 1H), 1.99 (p, *J* = 3.1 Hz, 3H), 1.86 – 1.54 (m, 15H), 1.35 – 1.19 (m, 7H).

$^{13}$C NMR (126 MHz, $CDCl_3$) δ 163.23, 149.30, 146.65, 138.04, 129.10, 128.73, 126.81, 45.66, 41.57, 36.84, 36.40, 33.98, 32.02, 31.53, 29.79, 28.54, 25.50, 18.92, 0.09.

**(3-((2-(Adamant-2-yl)ethyl)thio)-1*H*-1,2,4-triazol-1-yl)(2-benzylpiperidin-1-yl)methanone (28b)**

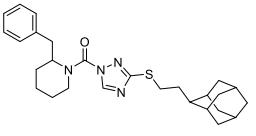

2-Benzylpiperidine (1.5 eq, 10 mg, 0.057 mmol) and **26b** (1 eq, 10 mg, 0.038 mmol) were coupled according to General procedure F to obtain the title compound as a white solid (11 mg, 0.024 mmol, 62%).

$^1$H NMR (500 MHz, $CDCl_3$) δ 8.12 (bs, 1H), 7.27 – 7.16 (m, 3H), 7.16 – 7.02 (m, 2H), 5.02 – 4.81 (m, 1H), 4.42 – 4.18 (m, 1H), 3.24 (td, *J* = 13.4, 2.8 Hz, 1H), 3.18 – 3.05 (m, 3H), 2.90 – 2.70 (m, 1H), 1.93 – 1.48 (m, 18H), 1.32 – 1.21 (m, 7H).

$^{13}$C NMR (126 MHz, $CDCl_3$) δ 162.41, 149.33, 146.98, 138.06, 129.15, 128.78, 126.87, 55.81 (br), 43.89 (br), 41.23, 39.19, 38.42, 36.44, 32.77, 31.85, 31.81, 31.79, 31.70, 30.37, 29.84, 28.32, 28.10, 25.55, 18.97, 14.27.

**(2-Benzylpiperidin-1-yl)(3-((cuban-1-ylmethyl)thio)-1*H*-1,2,4-triazol-1-yl)methanone (28c)**

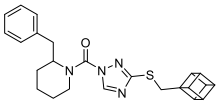

2-Benzylpiperidine (1.5 eq, 12 mg, 0.069 mmol) and **26c** (1 eq, 10 mg, 0.046 mmol) were coupled according to General procedure F to obtain the title compound as a white solid (12 mg, 0.029 mmol, 62%).

$^1$H NMR (500 MHz, $CDCl_3$) δ 8.08 (bs, 1H), 7.26 – 7.01 (m, 5H), 4.96 – 4.82 (m, 1H), 4.38 – 4.22 (m, 1H), 4.05 – 3.99 (m, 1H), 3.90 – 3.80 (m, 6H), 3.49 (d, *J* = 2.0 Hz, 2H), 3.24 (td, *J* = 13.3, 2.8 Hz, 1H), 3.20 – 3.10 (m, 1H), 2.88 – 2.73 (m, 1H), 1.86 – 1.51 (m, 3H), 1.28 – 1.23 (m, 4H).

$^{13}$C NMR (126 MHz, $CDCl_3$) δ 162.57, 149.28, 146.83, 138.09, 129.18, 128.77, 126.87, 55.57 (br), 48.79, 48.69, 44.07, 41.48 (br), 36.42, 35.36, 29.84, 27.30, 25.55, 22.84, 18.96.

**(3-(((Adamant-1-yl)methyl)thio)-1*H*-1,2,4-triazol-1-yl)(2-phenylpiperidin-1-yl)methanone (28d)**

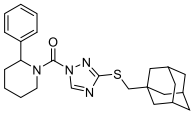

**27** (1.5 eq, 10 mg, 0.060 mmol) and **26a** (1 eq, 10 mg, 0.040 mmol) were coupled according to General procedure F to obtain the title compound as a white solid (12 mg, 0.027 mmol, 69%).

$^1$H NMR (500 MHz, $CDCl_3$) δ 8.74 (s, 1H), 7.43 – 7.32 (m, 4H), 7.32 – 7.27 (m, 1H), 5.97 – 5.87 (m, 1H), 4.42 – 4.32 (m, 1H), 3.02 (td, *J* = 13.3, 3.0 Hz, 1H), 2.88 (s, 2H), 2.52 – 2.44 (m, 1H), 2.09 – 1.98 (m, 1H), 1.96 – 1.91 (m, 3H), 1.82 – 1.54 (m, 11H), 1.52 – 1.45 (m, 6H).

$^{13}$C NMR (126 MHz, $CDCl_3$) δ 164.05, 149.64, 147.51, 138.20, 128.98, 127.18, 126.85, 56.41 (br), 45.45, 42.93 (br), 41.45, 36.83, 33.83, 28.52, 28.10, 25.77, 19.52.

**(3-((2-(Adamant-2-yl)ethyl)thio)-1*H*-1,2,4-triazol-1-yl)(2-phenylpiperidin-1-yl)methanone (28e)**

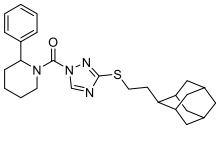

**27** (1.6 eq, 9 mg, 0.06 mmol) and **26b** (1 eq, 10 mg, 0.038 mmol) were coupled according to General procedure F to obtain the title compound as a white solid (12 mg, 0.027 mmol, 70%).

$^1$H NMR (500 MHz, $CDCl_3$) δ 8.76 (s, 1H), 7.41 – 7.32 (m, 4H), 7.31 – 7.27 (m, 1H), 6.00 – 5.84 (m, 1H), 4.46 – 4.33 (m, 1H), 3.10 – 2.92 (m, 3H), 2.52 – 2.44 (m, 1H), 2.10 – 1.98 (m, 1H), 1.90 – 1.58 (m, 19H), 1.53 – 1.45 (m, 2H).

$^{13}$C NMR (126 MHz, $CDCl_3$) δ 163.23, 149.62, 147.67, 138.21, 128.94, 127.17, 126.81, 56.27 (br), 43.75 (br), 43.05, 39.16, 38.40, 32.45, 31.75, 31.71, 31.67, 30.20, 28.31, 28.07, 28.00, 25.78, 19.50.

**(2-Phenylpiperidin-1-yl)(3-((cuban-1-ylmethyl)thio)-1*H*-1,2,4-triazol-1-yl)methanone (28f)**

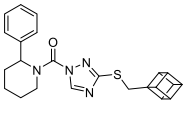

**27** (1.5 eq, 11 mg, 0.069 mmol) and **26c** (1 eq, 10 mg, 0.046 mmol) were coupled according to General procedure F to obtain the title compound as a white solid (16 mg, 0.030 mmol, 64%).

$^1$H NMR (500 MHz, $CDCl_3$) δ 8.75 (s, 1H), 7.41 – 7.32 (m, 4H), 7.31 – 7.27 (m, 1H), 5.94 – 5.84 (m, 1H), 4.43 – 4.32 (m, 1H), 4.03 – 3.96 (m, 1H), 3.86 – 3.80 (m, 3H), 3.80 – 3.73 (m, 3H), 3.36 (s, 2H), 3.03 (td, *J* = 13.4, 2.8 Hz, 1H), 2.52 – 2.44 (m, 1H), 2.10 – 1.99 (m, 1H), 1.81 – 1.59 (m, 4H).

$^{13}$C NMR (126 MHz, $CDCl_3$) δ 163.35, 149.60, 147.58, 138.23, 128.93, 127.15, 126.81, 56.34 (br), 48.75, 48.65, 44.01, 43.06 (br), 35.13, 28.03, 25.75, 19.49.

**(3-(((Adamant-1-yl)methyl)thio)-1*H*-1,2,4-triazol-1-yl)(morpholino)methanone (28g)**

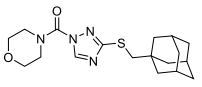

4-Morpholinecarbonyl chloride (2 eq, 12 mg, 0.080 mmol) and **26a** (1 eq, 10 mg, 0.040 mmol) were coupled according to General procedure G to obtain the title compound as a white solid (5 mg, 0.01 mmol, 34%).

$^1$H NMR (500 MHz, $CDCl_3$) δ 8.71 (s, 1H), 4.10 – 3.67 (m, 4H), 3.82 – 3.76 (m, 4H), 3.03 (s, 2H), 1.99 (p, *J* = 3.1 Hz, 3H), 1.75 – 1.55 (m, 12H).

$^{13}$C NMR (126 MHz, $CDCl_3$) δ 164.37, 148.41, 147.40, 66.74, 46.77 (br), 45.74, 41.66, 36.85, 33.93, 29.85, 28.55.

**(3-((2-(Adamant-2-yl)ethyl)thio)-1*H*-1,2,4-triazol-1-yl)(morpholino)methanone (28h)**

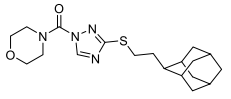

4-Morpholinecarbonyl chloride (2 eq, 11 mg, 0.076 mmol) and **26b** (1 eq, 10 mg, 0.038 mmol) were coupled according to General procedure G to obtain the title compound as a white solid (9 mg, 0.02 mmol, 55%).

$^1$H NMR (500 MHz, $CDCl_3$) δ 8.73 (s, 1H), 4.18 – 3.58 (m, 4H), 3.81 – 3.76 (m, 4H), 3.15 – 3.09 (m, 2H), 1.92 – 1.69 (m, 17H), 1.56 – 1.49 (m, 2H).

$^{13}$C NMR (126 MHz, $CDCl_3$) δ 163.59, 148.37, 147.67, 66.73, 46.75 (br), 43.93, 39.17, 38.38, 32.75, 31.78, 30.30, 28.29, 28.07.

**(3-((Cuban-1-ylmethyl)thio)-1*H*-1,2,4-triazol-1-yl)(morpholino)methanone (28i)**

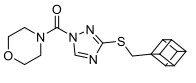

4-Morpholinecarbonyl chloride (14 mg, 0.092 mmol) and **26c** were coupled according to General procedure G to obtain the title compound as a white solid (13 mg, 0.038 mmol, 41%).

$^1$H NMR (500 MHz, $CDCl_3$) δ 8.73 (s, 1H), 4.06 – 3.99 (m, 1H), 4.08 – 3.70 (m, 4H), 3.90 – 3.85 (m, 3H), 3.85 – 3.81 (m, 3H), 3.81 – 3.76 (m, 4H), 3.49 (s, 2H).

$^{13}$C NMR (126 MHz, $CDCl_3$) δ 163.68, 148.32, 147.52, 66.72, 57.02, 48.78, 48.66, 46.98 (br), 44.06, 35.34.

## References


1. Landa, S. & Macháček, V. Sur l'adamantane, nouvel hydrocarbure extrait du naphte. *Collect. Czechoslov. Chem. Commun.* **5**, 1–5 (1933).
2. Lamoureux, G. & Artavia, G. Use of the Adamantane Structure in Medicinal Chemistry. *Curr. Med. Chem.* **17**, 2967–2978 (2010).
3. Wanka, L., Iqbal, K. & Schreiner, P. R. The lipophilic bullet hits the targets: Medicinal chemistry of adamantane derivatives. *Chem. Rev.* **113**, 3516–3604 (2013).
4. Dahl, J. E., Liu, S. G. & Carlson, R. M. K. Isolation and structure of higher diamondoids, nanometer-sized diamond molecules. *Science (80-. ).* **299**, 96–99 (2003).
5. Schleyer, P. V. R. A Simple Preparation of Adamantane. *J. Am. Chem. Soc.* **79**, 3292 (1957).
6. Liu, J., Obando, D., Liao, V., Lifa, T. & Codd, R. The many faces of the adamantyl group in drug design. *Eur. J. Med. Chem.* **46**, 1949–1963 (2011).
7. Reisberg, B. *et al.* Memantine in Moderate-to-Severe Alzheimer's Disease. *N. Engl. J. Med.* **348**, 1333–1341 (2003).
8. Rosenthal, K. S., Sokol, M. S., Ingram, R. L., Subramanian, R. & Fort, R. C. Tromantadine: inhibitor of early and late events in herpes simplex virus replication. *Antimicrob. Agents Chemother.* **22**, 1031–1036 (1982).
9. Ickes, D. E., Venetta, T. M., Phonphok, Y. & Rosenthal, K. S. Tromantadine inhibits a late step in herpes simplex virus type 1 replication and syncytium formation. *Antiviral Res.* **14**, 75–85 (1990).
10. Balzarini, J., Orzeszko-Krzesińska, B., Maurin, J. K. & Orzeszko, A. Synthesis and anti-HIV studies of 2- and 3-adamantyl-substituted thiazolidin-4-ones. *Eur. J. Med. Chem.* **44**, 303–311 (2009).
11. Balzarini, J., Orzeszko, B., Maurin, J. K. & Orzeszko, A. Synthesis and anti-HIV studies of 2-adamantyl-substituted thiazolidin-4-ones. *Eur. J. Med. Chem.* **42**, 993–1003 (2007).
12. Barnett, A. DPP-4 inhibitors and their potential role in the management of type 2 diabetes. *Int. J. Clin. Pract.* **60**, 1454–1470 (2006).
13. Kim, I. H., Morisseau, C., Watanabe, T. & Hammock, B. D. Design, Synthesis, and Biological Activity of 1,3-Disubstituted Ureas as Potent Inhibitors of the Soluble Epoxide Hydrolase of Increased Water Solubility. *J. Med. Chem.* **47**, 2110–2122 (2004).
14. Kasuga, J. *et al.* SAR-oriented discovery of peroxisome proliferator-activated receptor pan agonist with a 4-adamantylphenyl group as a hydrophobic tail. *Bioorg. Med. Chem. Lett.* **18**, 1110–1115 (2008).
15. Wennekes, T. *et al.* Synthesis and evaluation of dimeric lipophilic iminosugars as inhibitors of glucosylceramide metabolism. *Tetrahedron: Asymmetry* **20**, 836–846 (2009).
16. Wennekes, T. *et al.* Development of adamantan-1-yl-methoxy-functionalized 1-deoxynojirimycin derivatives as selective inhibitors of glucosylceramide metabolism in man. *J. Org. Chem.* **72**, 1088–1097 (2007).
17. Overkleeft, H. S. *et al.* Generation of Specific Deoxynojirimycin-type Inhibitors of the Non-lysosomal Glucosylceramidase. *J. Biol. Chem.* **273**, 26522–26527 (1998).
18. Mylvaganam, M. & Lingwood, C. A. Adamantyl Globotriaosyl Ceramide: A Monovalent Soluble Mimic Which Inhibits Verotoxin Binding to Its Glycolipid Receptor. *Biochem. Biophys. Res. Commun.* **257**, 391–394 (1999).
19. Tsuzuki, N. *et al.* Adamantane as a Brain-Directed Drug Carrier for Poorly Absorbed Drug. 2. AZT Derivatives Conjugated with the 1-Adamantane Moiety. *J. Pharm. Sci.* **83**, 481–484 (1994).
20. Lu, D. *et al.* Adamantyl cannabinoids: A novel class of cannabinergic ligands. *J. Med. Chem.* **48**, 4576–4585 (2005).

21. Jia, L. *et al.* Pharmacodynamics and pharmacokinetics of SQ109, a new diamine-based antitubercular drug. *Br. J. Pharmacol.* **144**, 80–87 (2005).
22. Kaur, G. *et al.* Synthesis, structure–activity relationship, and p210bcr-abl protein tyrosine kinase activity of novel AG 957 analogs. *Bioorg. Med. Chem.* **13**, 1749–1761 (2005).
23. Bodor, N., El-Koussi, A. A., Khalifa, M. M. & Kano, M. Soft Drugs. 7. Soft β-Blockers for Systemic and Ophthalmic Use. *J. Med. Chem.* **31**, 1651–1656 (1988).
24. Rapala, R. T., Kraay, R. J. & Gerzon, K. The Adamantyl Group in Medicinal Agents. II. Anabolic Steroid I7β-Adamantoates. *J. Med. Chem.* **8**, 580–583 (1965).
25. Gerzon, I. & Kau, D. The Adamantyl Group in Medicinal Agents. III. Nucleoside 5′-Adamantoates. The Adamantoyl Function as a Protecting Group1. *J. Med. Chem.* **10**, 189–199 (1967).
26. Masereel, B., Rolin, S., Abbate, F., Scozzafava, A. & Supuran, C. T. Carbonic anhydrase inhibitors: Anticonvulsant sulfonamides incorporating valproyl and other lipophilic moieties. *J. Med. Chem.* **45**, 312–320 (2002).
27. Gerzon, K., Krumkalns, E. V., Brindle, R. L., Marshall, F. J. & Root, M. A. The Adamantyl Group in Medicinal Agents. I. Hypoglycemic *N*-Arylsulfonyl-*N*′-adamantylureas. *J. Med. Chem.* **6**, 760–763 (1963).
28. Reekie, T. A., Williams, C. M., Rendina, L. M. & Kassiou, M. Cubanes in Medicinal Chemistry. *J. Med. Chem.* **62**, 1078–1095 (2019).
29. Auberson, Y. P. *et al.* Improving Nonspecific Binding and Solubility: Bicycloalkyl Groups and Cubanes as para-Phenyl Bioisosteres. *ChemMedChem* **12**, 590–598 (2017).
30. Wlochal, J., Davies, R. D. M. & Burton, J. Cubanes in medicinal chemistry: Synthesis of functionalized building blocks. *Org. Lett.* **16**, 4094–4097 (2014).
31. Long, J. Z. & Cravatt, B. F. The Metabolic Serine Hydrolases and Their Functions in Mammalian Physiology and Disease. *Chem. Rev.* **111**, 6022–6063 (2011).
32. Bachovchin, D. A. & Cravatt, B. F. The pharmacological landscape and therapeutic potential of serine hydrolases. *Nat. Rev. Drug Discov.* **11**, 52–68 (2012).
33. Faucher, F., Bennett, J. M., Bogyo, M. & Lovell, S. Strategies for Tuning the Selectivity of Chemical Probes that Target Serine Hydrolases. *Cell Chem. Biol.* **27**, 937–952 (2020).
34. Baggelaar, M. P., Maccarrone, M. & van der Stelt, M. 2-Arachidonoylglycerol: A signaling lipid with manifold actions in the brain. *Prog. Lipid Res.* **71**, 1–17 (2018).
35. Kozak, K. R. & Marnett, L. J. Oxidative metabolism of endocannabinoids. *Prostaglandins Leukot. Essent. Fat. Acids* **66**, 211–220 (2002).
36. Hu, S. S. J., Bradshaw, H. B., Chen, J. S. C., Tan, B. & Walker, J. M. Prostaglandin $E_2$ glycerol ester, an endogenous COX-2 metabolite of 2-arachidonoylglycerol, induces hyperalgesia and modulates NFκB activity. *Br. J. Pharmacol.* **153**, 1538–1549 (2008).
37. Murataeva, N., Straiker, A. & MacKie, K. Parsing the players: 2-arachidonoylglycerol synthesis and degradation in the CNS. *Br. J. Pharmacol.* **171**, 1379–1391 (2014).
38. van Esbroeck, A. C. M. *et al.* Identification of α,β-Hydrolase Domain Containing Protein 6 as a Diacylglycerol Lipase in Neuro-2a Cells. *Front. Mol. Neurosci.* **12**, (2019).
39. Straiker, A. *et al.* COX-2 and fatty acid amide hydrolase can regulate the time course of depolarization-induced suppression of excitation. *Br. J. Pharmacol.* **164**, 1672–1683 (2011).
40. Buisseret, B., Alhouayek, M., Guillemot-Legris, O. & Muccioli, G. G. Endocannabinoid and Prostanoid Crosstalk in Pain. *Trends Mol. Med.* **25**, 882–896 (2019).
41. Marrs, W. R. *et al.* The serine hydrolase ABHD6 controls the accumulation and efficacy of 2-AG at cannabinoid receptors. *Nat. Neurosci.* **13**, 951–957 (2010).

42. Alhouayek, M., Masquelier, J., Cani, P. D., Lambert, D. M. & Muccioli, G. G. Implication of the anti-inflammatory bioactive lipid prostaglandin $D_2$-glycerol ester in the control of macrophage activation and inflammation by ABHD6. *Proc. Natl. Acad. Sci.* **110**, 17558–17563 (2013).
43. Tchantchou, F. & Zhang, Y. Selective inhibition of alpha/beta-hydrolase domain 6 attenuates neurodegeneration, alleviates blood brain barrier breakdown, and improves functional recovery in a mouse model of traumatic brain injury. *J. Neurotrauma* **30**, 565–579 (2013).
44. Manterola, A. *et al.* Re-examining the potential of targeting ABHD6 in multiple sclerosis: Efficacy of systemic and peripherally restricted inhibitors in experimental autoimmune encephalomyelitis. *Neuropharmacology* **141**, 181–191 (2018).
45. Wen, J., Ribeiro, R., Tanaka, M. & Zhang, Y. Activation of $CB_2$ receptor is required for the therapeutic effect of ABHD6 inhibition in experimental autoimmune encephalomyelitis. *Neuropharmacology* **99**, 196–209 (2015).
46. Manterola, A. *et al.* Deregulation of the endocannabinoid system and therapeutic potential of ABHD6 blockade in the cuprizone model of demyelination. *Biochem. Pharmacol.* **157**, 189–201 (2018).
47. Tanaka, M. *et al.* WWL70 attenuates $PGE_2$ production derived from 2-arachidonoylglycerol in microglia by ABHD6-independent mechanism. *J. Neuroinflammation* **14**, 7 (2017).
48. Blankman, J. L., Long, J. Z., Trauger, S. A., Siuzdak, G. & Cravatt, B. F. ABHD12 controls brain lysophosphatidylserine pathways that are deregulated in a murine model of the neurodegenerative disease PHARC. *Proc. Natl. Acad. Sci.* **110**, 1500–1505 (2013).
49. Kamat, S. S. *et al.* Immunomodulatory lysophosphatidylserines are regulated by ABHD16A and ABHD12 interplay. *Nat. Chem. Biol.* **11**, 164–171 (2015).
50. Singh, S., Joshi, A. & Kamat, S. S. Mapping the Neuroanatomy of ABHD16A, ABHD12, and Lysophosphatidylserines Provides New Insights into the Pathophysiology of the Human Neurological Disorder PHARC. *Biochemistry* **59**, 2299–2311 (2020).
51. Deng, H. & Li, W. Therapeutic potential of targeting α/β-Hydrolase domain-containing 6 (ABHD6). *Eur. J. Med. Chem.* **198**, (2020).
52. Ogasawara, D. *et al.* Rapid and profound rewiring of brain lipid signaling networks by acute diacylglycerol lipase inhibition. *Proc. Natl. Acad. Sci.* **113**, 26–33 (2016).
53. Hsu, K. L. *et al.* Discovery and optimization of piperidyl-1,2,3-triazole ureas as potent, selective, and in vivo-active inhibitors of α/β-hydrolase domain containing 6 (ABHD6). *J. Med. Chem.* **56**, 8270–8279 (2013).
54. Janssen, A. P. A. Hit-to-Lead Optimization of Triazole Sulfonamide DAGL-α inhibitors. *Inhibitor Selectivity: Profiling and Prediction* (Leiden University, 2019).
55. Janssen, F. J. Discovery of 1,2,4-triazole sulfonamide ureas as in vivo active α/β hydrolase domain type 16A inhibitors. *Discovery of novel inhibitors to investigate diacylglycerol lipases and α/β hydrolase domain 16A* (Leiden University, 2016).
56. Deng, H. *et al.* Triazole Ureas Act as Diacylglycerol Lipase Inhibitors and Prevent Fasting-Induced Refeeding. *J. Med. Chem.* **60**, 428–440 (2017).
57. Cravatt, B. F. *et al.* Molecular characterization of an enzyme that degrades neuromodulatory fatty-acid amides. *Nature* **384**, 83–87 (1996).
58. Katritzky, A. R., Darabantu, M., Aslan, D. C. & Oniciu, D. C. Selective Reactivity of sp3and sp2 Carbanions of 1-Substituted 1,2,4-Triazoles. A Comparative Approach. *J. Org. Chem.* **63**, 4323–4331 (1998).
59. Hsu, K. L. *et al.* DAGLβ inhibition perturbs a lipid network involved in macrophage inflammatory responses. *Nat. Chem. Biol.* **8**, 999–1007 (2012).

60. Van Esbroeck, A. C. M. *et al.* Activity-based protein profiling reveals off-target proteins of the FAAH inhibitor BIA 10-2474. *Science* **356**, 1084–1087 (2017).
61. Liu, Y., Patricelli, M. P. & Cravatt, B. F. Activity-based protein profiling: The serine hydrolases. *Proc. Natl. Acad. Sci.* **96**, 14694–14699 (1999).
62. Pfeiffer, R. F., Wszolek, Z. K. & Ebadi, M. *Parkinson's disease, second edition*. *Parkinson's Disease, Second Edition* (CRC Press, 2012). doi:10.1201/b12948.
63. Hsu, K. L. *et al.* Development and optimization of piperidyl-1,2,3-triazole ureas as selective chemical probes of endocannabinoid biosynthesis. *J. Med. Chem.* **56**, 8257–8269 (2013).
64. Gopalan, B. *et al.* Discovery of adamantane based highly potent HDAC inhibitors. *Bioorganic Med. Chem. Lett.* **23**, 2532–2537 (2013).

# Supplementary information

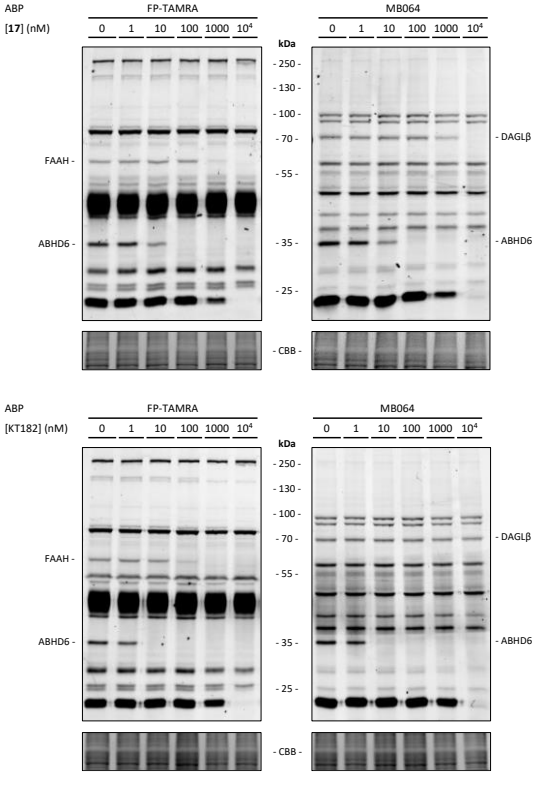


**Supplementary Figure S6.1. Full gel images of cellular cABPP assays.** Representative fluorescence images and coomassie protein loading controls of cABPP experiments on Neuro-2a cells, shown for compound **17** (A) and KT182 (B). Activity-based probes (ABPs) used are indicated, as well as intended inhibitor target and most relevant off-targets.

**Supplementary Table S6.1. *In vitro* inhibitory activity of 13–21 and KT182 on mouse brain enzymes.** $pIC_{50}$ values (left column for each inhibitor) determined from cABPP experiments on mouse brain proteome with probes FP-TAMRA and MB064. Data presented as mean ± SEM (N = 3). For each inhibitor the apparent fold selectivity (app. sel.) on its intended target (indicated with "–") over its respective off-targets is stated in the right column.

| | 13 | | 14 | | 15 | | 16 | | 17 | | 18 | | KT182 | | 19 | | 20 | | 21 | |
|---|---|---|---|---|---|---|---|---|---|---|---|---|---|---|---|---|---|---|---|---|
| | $pIC_{50}$ ± SEM | App. sel. | $pIC_{50}$ ± SEM | App. sel. | $pIC_{50}$ ± SEM | App. sel. | $pIC_{50}$ ± SEM | App. sel. | $pIC_{50}$ ± SEM | App. sel. | $pIC_{50}$ ± SEM | App. sel. | $pIC_{50}$ ± SEM | App. sel. | $pIC_{50}$ ± SEM | App. sel. | $pIC_{50}$ ± SEM | App. sel. | $pIC_{50}$ ± SEM | App. sel. |
| **ABHD6** | 6.49 ± 0.07 | 17 | 7.05 ± 0.03 | 3.4 | 6.84 ± 0.06 | 14 | 6.49 ± 0.05 | – | 6.80 ± 0.03 | – | 6.61 ± 0.05 | – | 7.40 ± 0.04 | – | 7.53 ± 0.05 | < 1 | 7.82 ± 0.03 | < 1 | 7.26 ± 0.07 | < 1 |
| **ABHD12** | < 5.0 | > 537 | < 5.0 | > 380 | < 5.0 | > 1000 | < 5.0 | > 30 | < 5.0 | > 63 | < 5.0 | > 40 | < 5.0 | > 251 | 5.44 ± 0.19 | 39 | 6.29 ± 0.11 | 18 | 5.47 ± 0.14 | 7.8 |
| **ABHD16a** | < 5.0 | > 537 | < 5.0 | > 380 | < 5.0 | > 1000 | < 5.0 | > 30 | < 5.0 | > 63 | < 5.0 | > 40 | < 5.0 | > 251 | 7.03 ± 0.07 | – | 7.55 ± 0.04 | – | 6.36 ± 0.07 | – |
| **DAGLα** | 7.73 ± 0.08 | – | 7.58 ± 0.09 | – | 8.00 ± 0.06 | – | 5.60 ± 0.08 | 7.8 | 5.68 ± 0.06 | 13 | 6.00 ± 0.07 | 4.1 | < 5.0 | > 251 | 5.44 ± 0.19 | 39 | 5.75 ± 0.13 | 63 | 4.91 ± 0.24 | 28 |
| **DDHD2** | < 5.0 | > 537 | < 5.0 | > 380 | < 5.0 | > 1000 | < 5.0 | > 30 | < 5.0 | > 63 | < 5.0 | > 40 | < 5.0 | > 251 | 5.81 ± 0.08 | 17 | 5.64 ± 0.11 | 81 | < 5.0 | > 22 |
| **FAAH** | < 5.0 | > 537 | < 5.0 | > 380 | < 5.0 | > 1000 | < 5.0 | > 30 | < 5.0 | > 63 | 5.59 ± 0.06 | 10 | < 5.0 | > 251 | < 5.0 | > 107 | < 5.0 | > 354 | 5.64 ± 0.04 | 5.2 |
| **KIAA1363** | < 5.0 | > 537 | < 5.0 | > 380 | < 5.0 | > 1000 | < 5.0 | > 30 | < 5.0 | > 63 | < 5.0 | > 40 | < 5.0 | > 251 | < 5.0 | > 107 | < 5.0 | > 354 | < 5.0 | > 22 |
| **LyPLA1/2** | 5.20 ± 0.06 | 339 | < 5.0 | > 380 | < 5.0 | > 1000 | 6.86 ± 0.03 | < 1 | 6.04 ± 0.04 | 5.8 | 6.84 ± 0.02 | < 1 | 5.13 ± 0.05 | 186 | 7.03 ± 0.10 | 1 | 6.83 ± 0.08 | 5.2 | 6.42 ± 0.06 | < 1 |
| **MAGL** | < 5.0 | > 537 | < 5.0 | > 380 | < 5.0 | > 1000 | < 5.0 | > 30 | < 5.0 | > 63 | < 5.0 | > 40 | < 5.0 | > 251 | < 5.0 | > 107 | < 5.0 | > 354 | < 5.0 | > 22 |
| **NTE** | < 5.0 | > 537 | < 5.0 | > 380 | < 5.0 | > 1000 | < 5.0 | > 30 | < 5.0 | > 63 | < 5.0 | > 40 | 5.46 ± 0.15 | 87 | 5.03 ± 0.10 | 100 | 5.62 ± 0.15 | 85 | 5.27 ± 0.09 | 12 |